HgTe-CdTe superlattice subband dispersion

J. N. Schulman
Hughes Research Laboratories, Malibu, California 90265

Yia-Chung Chang
Department of Physics and Materials Research Laboratory, University of Illinois at Urbana-Champaign, Urbana, Illinois 61801

(Received 1 August 1985: revised manuscript received 5 November 1985)

The results of band-structure calculations for (001) and (111) HgTe-CdTe superlattices using a multiband tight-binding model are presented. The band structures of superlattices in the semiconducting and semimetallic regimes are found for directions both parallel and perpendicular to the growth direction. The tight-binding model automatically incorporates the correct space-group symmetry of the superlattice. Band mixing, band crossings or anticrossings, degeneracies, and spin splittings are therefore correctly produced. For semiconducting superlattices the strain-induced reversal of light- and heavy-hole subbands depends on growth orientation as well as layer thicknesses. The light-hole subband, as defined by the effective mass in the growth direction, is found to be higher than the heavy-hole subband for the (001) 50-Å–40-Å superlattice by 9.2 meV, but lower for the (111) superlattice with similar layer thicknesses. This feature is somewhat sensitive to the precise deformation potentials and bulk valence-band parameters assumed in the calculation. The semimetallic superlattice which had been the subject of magnetoabsorption experiments is studied in detail. In agreement with the calculation of Wu and McGill, it is found that the inclusion of strain significantly distorts the valence-band-edge band structure, implying that a reappraisal of the 40-meV HgTe-CdTe valence-band-offset determination is needed. It is found that the stress opens up a gap at the Brillouin-zone center, but that the superlattice is still semimetallic due to a stress-induced indirect valence-band maximum with energy above that of the conduction-band minimum. The conduction-band-minimum wave function has a large interfacial component. The relative magnitude of the amplitude of this component increases approximately with the inverse square root of the energy of the state.

I. INTRODUCTION

The HgTe-CdTe superlattice has been proposed as a new infrared-active material which may have certain advantages as compared with the Hg-Cd-Te alloy of the same band gap for long-wavelength (>12 μm) detection.[1,2] The molecular-beam-epitaxial growth of this superlattice in recent years has shown that material with good crystalline quality is available.[3,4] A series of theoretical and experimental investigations have begun to elucidate the electronic and optical properties of the superlattice. Experimental techniques used have included magneto-optical absorption,[5] the Hall effect,[6] infrared transmission,[6,7] and infrared luminescence.[8] Theoretical modeling has been done to calculate the band-gap dependence on layer thickness,[2,9] interdiffusion,[10] and temperature,[11] and other properties, including optical absorption,[12] strain effects,[13] and quasi-interface states,[14,15] have been studied.

There are many issues that must be investigated before the growing wealth of experimental data can be understood in terms of the theoretical models. One of the most important parameters to be determined is the valence-band offset between HgTe and CdTe. The early conjecture that it would be small,[1] based on the common anion rule, seems to have been confirmed by the magneto-optical absorption experiments in which a 40-meV offset was deduced.[5] Subsequent optical analyses of other superlattice samples are consistent with a small offset but do not specifically indicate 40 meV, or any other unique value of the offset.[4,7,8,16] The analysis is complicated by a variety of uncertainties, including layer-thickness determination, interdiffusion during growth, and interpretation of optical spectra, either from transmission or luminescence data. Since the magneto-optical experiment had the same complications, there is no basis for favoring the 40-meV value over those that would be implied by the other optical experiments. Determining the offset by adjusting it to fit the optically determined band gaps may be difficult, in general, since it has been shown that the band gap is not a very sensitive function of the offset, if the offset is small.[17]

Strain is another consideration complicating the analysis. There is a 0.3% lattice mismatch between CdTe and HgTe lattice constants (CdTe larger).[18] Wu and McGill[13] have included the effects of strain in a multiband $\mathbf{k}\cdot\mathbf{p}$ calculation. They have shown that, in common with other strained-layer superlattices, a reversal of the order in energy of the heavy- and light-hole subbands can occur. They point out that this would seriously affect the analysis of Ref. 5, since the heavy-hole subband was assumed higher in the analysis of the magneto-optical data, whereas including strain raises the light-hole subband higher.

The purpose of this paper is to report the results of a multiband tight-binding calculation which produces de-

tailed band structures for a variety of cases. Calculations for superlattices grown parallel to (001) and (111) orientations are similar but have noticeable differences which will be discussed. The dispersion of the energy bands both parallel and perpendicular to the growth direction will be shown. The tight-binding method has the advantage that the full space-group symmetry of the superlattice is incorporated. The correct degeneracies and spin splittings are therefore automatically produced. In Sec. II we describe the tight-binding model used, including the modifications for incorporating strain and the effects on the bulk band structures. In Sec. III we present the results for the semiconducting superlattice and in Sec. IV we present those for the semimetallic case. In Sec. V we discuss the interface nature of the conduction-band wave functions.

II. METHOD

A. Tight-binding method with strain

The tight-binding framework used in this calculation has been described previously. Without strain, it is identical to that presented in Ref. 19 for the GaAs-GaAlAs superlattice. It is a 20-band model, including spin, with three p-type and two s-type orbitals per atom and nearest-neighbor overlaps included. The tight-binding Schrödinger equation is solved using a basis consisting of HgTe and CdTe bulk states with complex wave vectors. This allows the calculation of band structures of superlattices with arbitrary unit-cell widths with the same computational effort, and provides a clear method for analyzing the superlattice electronic structure in relationship to those of the bulk band structures.[19]

The tight-binding parameters are listed in Table I. The bulk band gaps and effective masses produced by the parameters are given in Table II. Since only the band structure near the zone center is of interest in this paper, only zone-center quantities are listed. There is significant uncertainty in the literature concerning the values of the HgTe and CdTe effective masses or, equivalently, their Luttinger parameters.[20–23] The variation in published values is on the order of 25% for the light-hole masses. This introduces an uncertainty of the same order in the superlattice energies, which must be kept in mind when comparison with experiment is attempted. The heavy-hole masses have the additional complication of substantial anisotropy. Variations of over 100% in the ratio of [111] to [100] heavy-hole masses have been reported. The heavy effective mass makes this variation less important since the higher subbands are quite close to the HgTe valence-band edge in any case.

A valence-band offset of 40 meV was assumed consistent with the magneto-optical—absorption experiments.[5] As will be shown in Sec. IV, the theoretical analysis used to deduce this offset is probably inadequate, however. Nevertheless, it is consistent with the common anion-rule argument indicating an offset of zero. Although optical properties near the band gap may not depend sensitively on the offset,[17] transport properties should strongly depend on it. A critical area for future investigation is the value of the offset and its dependence on alloy composition, strain, and possibly temperature.

Strain is incorporated in a manner similar to that introduced by Osbourn for the GaAs-GaAsP strained-layer superlattice.[24] Additional tight-binding parameters are created which are determined to reproduce stress-induced energy shifts and splittings in the band structure. Osbourn incorporated stress effects on the light-hole, heavy-hole, direct conduction, and indirect conduction bands of both materials in his model. The situation is somewhat simpler here. First, the effect of stress on the CdTe layers is ignored. This is the case for thin enough superlattices grown on CdTe substrates or buffer layers. Only the HgTe layers are then stressed. It is not clear whether or not the superlattices that have been grown fall fully in this regime. If the CdTe layers were also strained, the strain on the HgTe layers would be decreased. In that case the calculations presented here would represent an overestimate of the effect of strain on the band structure. Second, only the shifts of the Γ_8 heavy-hole and (inverted) light-hole bands are considered since HgTe is direct and the negative-gap Γ_6 conduction band is out of the energy range of interest.

TABLE I. Empirical tight-binding parameters (in eV) for unstressed HgTe and CdTe. Notation is that of Ref. 34.

Parameter	HgTe	CdTe
$E_s(0,0,0)_a$	−8.0724	−8.1921
$E_p(0,0,0)_a$	0.4476	0.3279
$E_s(0,0,0)_c$	−3.5210	−0.9500
$E_p(0,0,0)_c$	5.0576	6.9379
$4E_{ss}(\frac{1}{2},\frac{1}{2},\frac{1}{2})$	−5.000	−5.000
$4E_{xx}(\frac{1}{2},\frac{1}{2},\frac{1}{2})$	2.0560	2.1360
$4E_{xy}(\frac{1}{2},\frac{1}{2},\frac{1}{2})$	5.3550	6.1855
$4E_{sx}(\frac{1}{2},\frac{1}{2},\frac{1}{2})_{ac}$	4.0031	4.0739
$4E_{sx}(\frac{1}{2},\frac{1}{2},\frac{1}{2})_{ca}$	5.608	6.242
$E_{s^*}(0,0,0)_a$	3.6556	10.4454
$E_{s^*}(0,0,0)_c$	9.4274	6.6296
$4E_{s^*x}(\frac{1}{2},\frac{1}{2},\frac{1}{2})_{ac}$	3.7688	4.3729
$4E_{s^*x}(\frac{1}{2},\frac{1}{2},\frac{1}{2})_{ca}$	5.6486	3.6986
Δ_a	1.0300	0.9680
Δ_c	0.8600	0.2270

TABLE II. Bulk band gaps (eV) and effective masses (in units of the electron mass) produced by the tight-binding parameters of Table I. (HH and LH denote heavy and light hole, respectively.)

	E_G	$m_C[001]$	$m_{HH}[001]$	$m_{LH}[001]$	$m_C[111]$	$m_{HH}[111]$	$m_{LH}[111]$
HgTe	−0.303	0.026	0.323	0.030	0.027	0.705	0.030
CdTe	1.602	0.087	0.323	0.088	0.087	0.656	0.077

Only one additional tight-binding parameter is then needed, a new parameter representing the overlap between p-type orbitals in certain orientations. The form and value of this parameter varies slightly depending on whether (001) or (111) superlattices are under consideration. The (001) case is simpler. The parameter E_{xx} in Table I represents overlaps between the same p-type orbital on the anion as on the cation (x-x, y-y, or z-z) separated by the nearest-neighbor distance. In the (001) strained-layer superlattice, the x-x and y-y values differ from the z-z value. The main effects of this breaking of symmetry are to cause a splitting of the bulk heavy-hole and light-hole Brillouin-zone—center energies and to shift them both.

The stressed HgTe heavy-hole and light-hole energy levels can be predicted from the known HgTe and CdTe lattice constants,[18] the HgTe elastic constants,[25] and the HgTe deformation potentials.[26] References 24 and 27 give formulas for the stress due to the lattice mismatch. In Bir-Pikus formalism, the stress (or strain) and the deformation potentials are used to calculate the energy levels.[28,29] The authors of Ref. 28 discuss zero-band-gap semiconductors in particular. The new tight-binding parameters are determined by adjusting them so that the hole energy levels as calculated by use of the Bir-Pikus model are produced.

The new (111) superlattice parameters are somewhat complicated because the p-type—orbital overlap parameters are defined relative to the conventional [001], [010]. and [100] axes. To see how the stress breaks symmetry, consider the bulk tight-binding Hamiltonian matrix between the p-type anion and cation orbitals (ϕ_x, ϕ_y, and ϕ_z). Let X be the $4E_{xx}$ parameter and Y the $4E_{xy}$ parameter. Then the matrix looks like[30]

$$H_{ac}=\begin{bmatrix} g_0X & g_3Y & g_2Y \\ g_3Y & g_0X & g_1Y \\ g_2Y & g_1Y & g_0X \end{bmatrix}, \tag{1}$$

where the rows are for the x, y, and z anion orbitals and the columns for the same cation orbitals. The g_i's are defined in Ref. 30.

TABLE III. Modified tight-binding parameter, $X=4E_{xx}(\frac{1}{2},\frac{1}{2},\frac{1}{2})$, and heavy-hole (HH) and light-hole (LH) Brillouin-zone zone-center energies (in eV) for stressed and unstressed HgTe. X^s is for the overlaps between orbitals directed along the [001] [for (001) superlattices] or [111] [for (111) superlattices] directions. X is for orbitals directed within the superlattice planes.

	X	X^s	E(HH)	E(LH)
Unstressed HgTe	2.0560	2.0560	0	0
(001) superlattice	2.0619	2.0129	−0.004	0.018
(111) superlattice	2.0456	2.01495	0.007	0.021

Equation (1) immediately shows that strain as found in the (001) superlattice is obtained by differentiating the X parameter in the $\langle\phi_z(a)\,|\,H_{ac}\,|\,\phi_z(c)\rangle$ matrix element from the X's in the $\langle\phi_x(a)\,|\,H_{ac}\,|\,\phi_x(c)\rangle$ and $\langle\phi_y(a)\,|\,H_{ac}\,|\,\phi_y(c)\rangle$ elements. The new values are labeled by X^s and X, respectively, in Table III.

It is useful to transform this matrix into a basis more natural for (111) superlattices. Let

$$\begin{aligned} \phi_1&=(\phi_x+\phi_y-2\phi_z)/\sqrt{6}\,, \\ \phi_2&=(\phi_x-\phi_y)/\sqrt{2}\,, \\ \phi_3&=(\phi_x+\phi_y+\phi_z)/\sqrt{3}\,. \end{aligned} \tag{2}$$

ϕ_3 is an orbital directed in the [111] direction, and ϕ_1 and ϕ_2 are directed in two directions perpendicular to ϕ_3. In this basis the matrix looks like

$$\bar{H}_{ac}=\begin{bmatrix} g_0X-(2g_1+2g_2-g_3)Y/3 & (g_1-g_2)/Y\sqrt{3} & -(g_1+g_2-2g_3)Y/\sqrt{18} \\ (g_1-g_2)Y/\sqrt{3} & g_0X-g_3Y & -(g_1-g_2)Y/\sqrt{6} \\ -(g_1+g_2-2g_3)Y/\sqrt{18} & -(g_1-g_2)Y/\sqrt{6} & g_0X+2(g_1+g_2+g_3)Y/3 \end{bmatrix}. \tag{3}$$

The simplest way to implement the strain-induced symmetry breaking for (111) superlattices is to differentiate the X tight-binding parameter in the $\langle\phi_3(a)\,|\,H\,|\,\phi_3(c)\rangle$ matrix element in Eq. (3) from the X parameters in the other matrix elements. Let it be represented by X^s. Both X and X^s take on new values with strain and are given in Table III. The Y parameter might also be modified, but this is found not to be necessary near the Brillouin-zone center. Since Y is multiplied by g_i factors which are zero at the zone center, it does not play as important a role as X. Transforming back to the ϕ_x,ϕ_y,ϕ_z basis gives

$$H^s_{ac}=\begin{bmatrix} g_0(2X+X^s)/3 & g_3Y-g_0(X-X^s)/3 & g_2Y-g_0(X-X^s)/3 \\ g_3Y-g_0(X-X^s)/3 & g_0(2X+X^s)/3 & g_1Y-g_0(X-X^s)/3 \\ g_2Y-g_0(X-X^s)/3 & g_1Y-g_0(X-X^s)/3 & g_0(2X+X^s)/3 \end{bmatrix}. \tag{4}$$

Similar overlap matrices are used for both the bulk and superlattice Hamiltonians. For the superlattice, there are two such matrices, one for interactions between the anion and its cation neighbor in the adjacent plane to the left and one for right interactions. Then, there are two g_i's, g_i^- and g_i^+. Their form can be found in Ref. 31.

B. Stressed bulk band structures

As discussed above, the two new parameter values are determined by reproducing the Bir-Pikus heavy-hole and light-hole energies. The two Brillouin-zone zone-center energies are used. They are given in Table III. The energy splittings and E_{xx} parameters are found to vary close to linearly with strain. Note that the shifts are different for the (001) and (111) superlattices.

Fitting only these energies produces an excellent agreement between the tight-binding bulk band structures and the Bir-Pikus band structures away from the Brillouin-zone center also. This can be seen in Fig. 1. Shown is the bulk HgTe band structure in the directions indicated as calculated with the tight-binding model. Only the Γ_8 bands are shown. Figure 1(b) includes tensile biaxial stress (HgTe has the smaller lattice constant) as occurs in the (001) superlattice. The effective masses in the [001] direction are relatively unaffected. The band with the light-hole mass in this direction is higher than the heavy-hole band, as given in Table III. The bands in the in-plane directions, [100] and [110], are modified significantly. The lower band acquires a light positive mass and thus an indirect valence-band maximum. This is due to the $\mathbf{k}\cdot\mathbf{p}$ repulsion from the negative-band-gap Γ_6 band, which is no longer forbidden by symmetry.[28] The upper band still has a positive mass, but it is flatter than the unstrained band. Figure 1(b) also shows the strained bands as calculated in the Bir-Pikus model. The major difference is that the spin splitting of the bands is not included.

The effects of stress illustrated here are similar to those shown in Ref. 28 for uniaxially compressed gray tin and to those described previously for the HgTe-CdTe superlattice in Ref. 13. The HgTe band structure relevant to the case of (111) superlattice stress is illustrated in Ref. 32. The same features are found as in this case. Osbourn has reported the results of a systematic theoretical study of effective masses in strained-layer superlattices.[33]

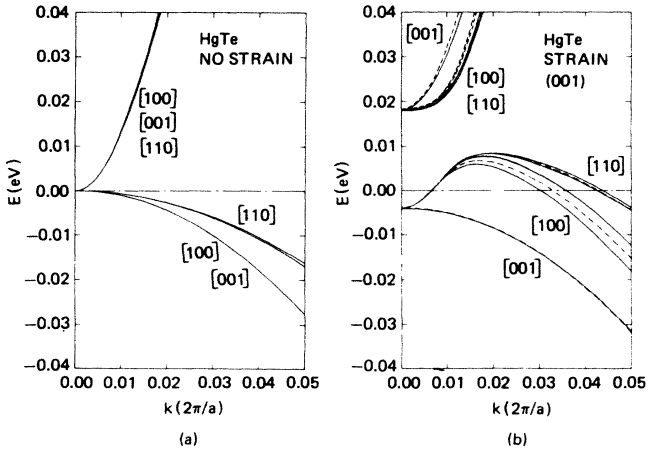

FIG. 1. Bulk HgTe band structure (a) without and (b) with strain as found in a (001) HgTe-CdTe superlattice. Solid line: tight-binding model. Dashed line: Bir-Pikus model. a is the HgTe lattice constant.

III. SEMICONDUCTING SUPERLATTICE

The HgTe-CdTe superlattice is predicted to be semiconducting or semimetallic depending on the HgTe and CdTe layer thicknesses.[9] Increasing the HgTe layer thickness lowers the band gap, and if the HgTe to CdTe layer-thickness ratio is high enough, the conduction band actually crosses the heavy-hole band, resulting in the semimetallic condition. This behavior is due to the unique quasi-interface-state nature of the conduction band and demonstrates the non-quantum-well-like behavior of the superlattice.[14,15] In this section the semiconducting case will be discussed.

The semiconducting superlattice discussed here is that fabricated and analyzed as reported in Ref. 6. It consisted of 50 Å of HgTe alternating with 40 Å of CdTe grown on a CdTe substrate oriented along the (111) plane. Since 50 and 40 Å do not represent integral numbers of layers, the calculation was done for a 48.6-Å–41.1-Å superlattice. An interesting experimental feature observed was a conversion from n to p type below a transition temperature of 150 K and a very high, (1.1×10^4)-cm^2/V s, p-type mobility at 10 K. It was speculated that the high mobility may have been due to a band-mixing effect between the heavy- and light-hole bands.[6]

Figure 2 shows the band structure of the superlattice in two directions: along the [111] axis (k_z), and within the (111) plane along the [11$\bar{2}$] direction (k_x). Note the different scales for k_z and k_x. The bands are approximately isotropic within the (111) plane. The zero of energy is chosen to be the HgTe degenerate valence- and conduction-band edge. The top band shown is the conduction band. It is derived from the HgTe inverted Γ_8 light-hole band and the CdTe light-hole band. Hopefully, confusion will not be introduced by referring to this conduction band as being light-hole-like in its atomic-orbital character. It is, of course, unoccupied at low temperature when undoped. The bands (a) without and (b) with strain included are given. Also shown are the bulk HgTe heavy-hole and (inverted) light-hole bands.

The k_z dispersion clearly identifies the character of the bands in this direction as being heavy- or light-hole-like. The inclusion of strain raises the energy of the light-hole valence band (second lowest band at the Brillouin-zone zone center) relative to the highest heavy-hole band slightly. The band gap is almost unchanged since both the conduction and highest heavy-hole band are raised. The effective masses in the [111] direction are substantially greater than the bulk masses.

The anisotropy in transport can be clearly seen, with the in-plane masses being much less than those in the [111] direction. The in-plane conduction mass is slightly heavier than the bulk mass. The in-plane dispersion is

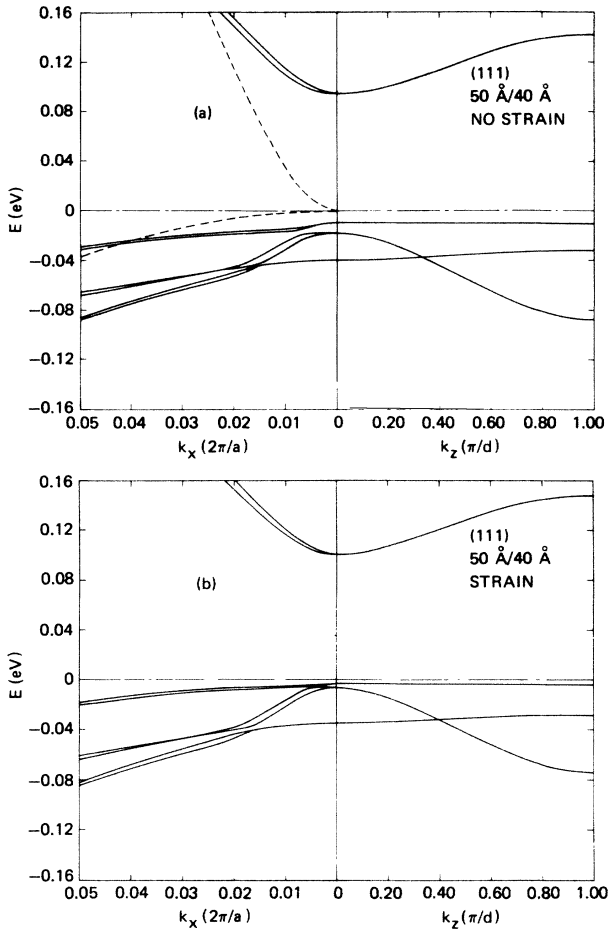

FIG. 2. Band structure of (111) 50-Å—40-Å HgTe-CdTe superlattice in [111] (k_z) and [11$\bar{2}$] (k_x) directions. (a) Without strain. (b) With strain. d is the width of the superlattice unit cell in the growth direction. The dashed lines are the bulk HgTe bands in the [111] direction.

complicated by several factors. The bands are no longer spin doubly degenerate. The splitting is due to the incorporation of the full space group by the tight-binding method and is not produced by simpler models such as the envelope function method. They include nonexistent mirror planes bisecting well and barrier layers. The splitting and the mixing of heavy-hole and light-hole character make the characterization of the bands difficult.

It is not clear whether or not the band structure shown in Fig. 2(a) contributes to an explanation for the observed high hole mobility, or especially the transition from n to p type below 150 K. A close examination of the highest valence band does reveal a decreased effective mass out to about $k_x \simeq 0.007(2\pi/a)$ over an energy range of ≈ 6 meV. The strained superlattice also has a decreased effective mass, but it occurs over such a small energy range (≈ 2 meV) that it is not resolvable in Fig. 2(b). Cade has also noticed a decreased valence-band mass for a 100-Å HgTe-CdTe quantum well.[15]

The band structure within such a small scale in energy and k_x is somewhat dependent on the input parameters of the calculation and the valence-band offset used. The problem of calculating superlattice hole mobilities based on the band structures is also far from trivial. The present results should be regarded as suggestive only until more systematic data and a more complete calculation of the superlattice mobility are available.

Repeating the calculation for a 48.5-Å—38.8-Å (001) superlattice results in the band structure shown in Fig. 3. The most important difference as compared to the (111) superlattice is that the light-hole valence band is raised by strain in energy enough to place it above the highest heavy-hole band. The separation in energy between the two is 9.2 meV. This is due to the fact that the bulk HgTe bands are shifted more by the (001) strained-layer effect than by the (111) strain. This can be seen by comparing the 22-meV (001) heavy-hole—light-hole splitting with the 14-meV (111) splitting in Table III. Transport in the growth direction, [001], would thereby be greater than otherwise expected at low temperatures. The k_x dispersion of the highest valence band shows no evidence of a decreased effective mass, unlike the case of the (111) superlattice.

The effect of the different space groups for the (111) and (001) superlattices can be seen by comparing the k_z dispersion in Figs. 2 and 3. C_{2v} is the symmetry group along the [001] direction for the (001) superlattice. There

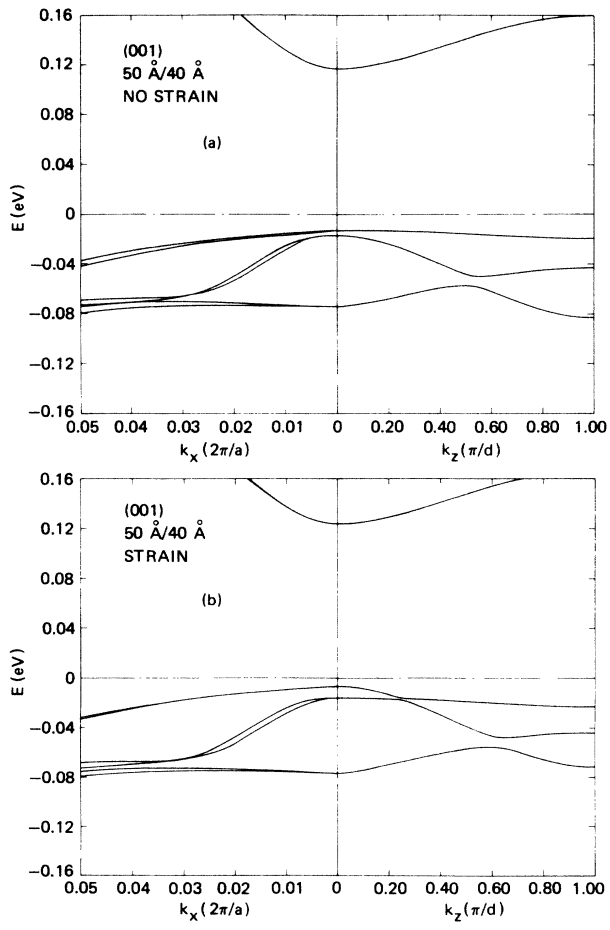

FIG. 3. Band structure of (001) 50-Å—40-Å HgTe-CdTe superlattice in [001] (k_z) and [100] (k_x) directions. (a) Without strain. (b) With strain.

is only one doubly degenerate double group irreducible representation and therefore the bands cannot cross and must repel (Fig. 3).[19] For (111) superlattices in the [111] direction, C_{3v} is the group. There are two doubly degenerate representations. One of them is doubly degenerate due to time reversal. The bands with two different representations can cross, as seen in Fig. 2.

IV. SEMIMETALLIC SUPERLATTICE

The band structure of a (111) 179.4-Å—44.8-Å superlattice is shown in Fig. 4. This is the same as that used for the magneto-optical—absorption measurements on the nominally 180-Å—44-Å superlattice of Ref. 5. Wu and McGill have previously calculated that stress reverses the order of the highest heavy- and light-hole subbands at the Brillouin-zone zone center for this case.[13] They assumed a valence-band offset of zero. The present tight-binding calculation using a 40-meV offset agrees with this conclusion.

The k_z dispersion shows that the unstrained superlattice is obviously semimetallic due to the intersection of the conduction band with two of the heavy-hole subbands. Although Ref. 5 also found the unstrained superlattice to be semimetallic, the conduction-band energy at the Brillouin-zone zone center was found to be almost degenerate with the highest heavy-hole subband. This discrepancy is not due to the differences between the tight-binding formalism used here and the envelope-function approach of Ref. 5, but between the actual values of the bulk CdTe light-hole masses assumed in fitting the empirical parameters in the two calculations. When the same bulk effective masses and band gaps are assumed, there is very good agreement between the two models concerning the Brillouin-zone zone-center energy levels for the lower indexed subbands. A CdTe mass of $0.16m_e$ is implied by the band gaps and momentum matrix elements of Ref. 5, whereas Table II gives $0.077m_e$ as the value produced by the tight-binding parameters assumed here. These two values are near the high and low values found in the literature, but are not unrepresentative. A lower CdTe mass does decrease the conduction-band energy, however, and since $0.16m_e$ is a significantly larger than average value, it seems likely that the conduction band would intersect at least one of the heavy-hole subbands.

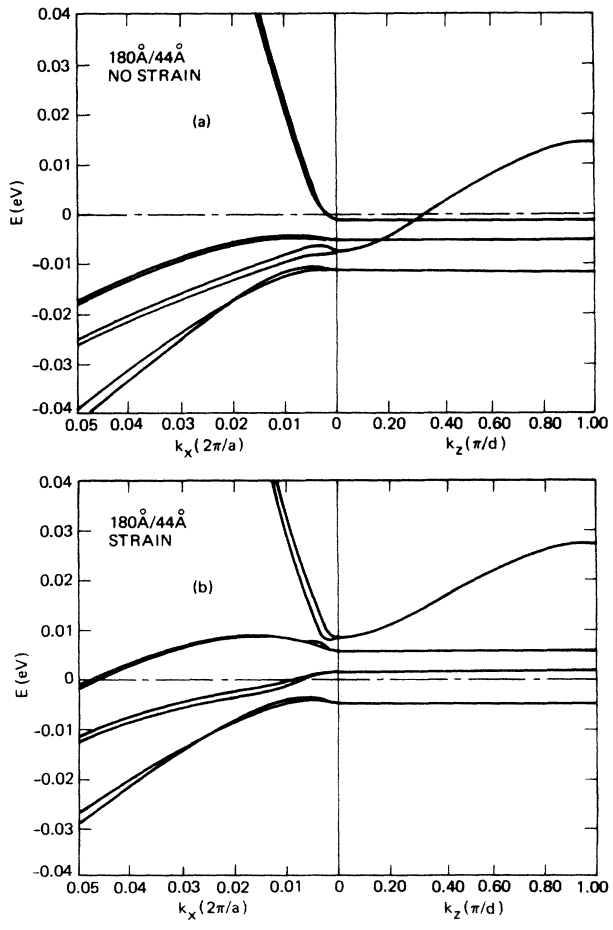

FIG. 4. Band structure of (111) 180-Å—44-Å HgTe-CdTe superlattice in [111] (k_z) and [11$\bar{2}$] (k_x) directions. (a) Without strain. (b) With strain.

The modification of the bands by strain are shown in Fig. 4(b). The k_z dispersion reveals that in this case also the conduction band (with light-hole orbital character) is raised above the heavy-hole band, seeming to open up a gap. The k_x dispersion shows that this is not the case. The strain-induced repulsion of the highest valence band from the lower bands has caused it to attain an indirect valence-band maximum which is actually higher than the conduction-band minimum. It is again semimetallic. The Fermi level would lie between the valence-band maximum and conduction-band minimum. Strain is not included in the analysis of Ref. 5. Since the effective masses and the location of the Fermi level are seen to be modified significantly by strain, the deduced 40-meV offset should be reexamined.

V. INTERFACE CHARACTER

HgTe-CdTe superlattices have been predicted to have conduction-band wave functions which have large amplitudes at the HgTe-CdTe interfaces.[14,15] This is due to the coupling of the inverted positive-mass Γ_8 conduction band in HgTe with the normal negative-mass Γ_8 light-hole band in CdTe.

The lowest conduction-band wave function at the Brillouin-zone zone center has two major components whose relative contributions depend on the energy of the state relative to the HgTe conduction-band minimum. The smaller component is the familiar Kronig-Penney—like cosine function. It is similar to the type of wave function found for conduction-band states of the GaAs-GaAlAs superlattice. In terms of atomic orbitals, the component is found on the cation s orbitals. The larger component is peaked at the interfaces. The change in sign of the bulk effective mass there produces a change in sign of the slope of the wave function, and thus a cusp. It is found on the anion p orbitals.

The envelope-function method provides a simple estimate of the relative sizes of the two components. The wave function is described in terms of F_s and F_p, where

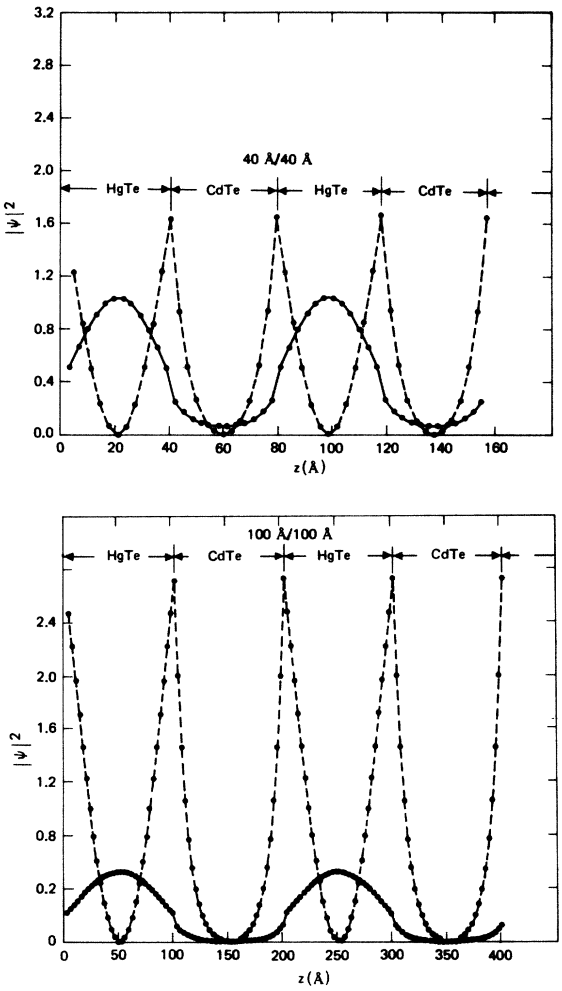

FIG. 5. Squared wave functions for 40-Å—40-Å and 100-Å—100-Å HgTe-CdTe superlattices. Two unit cells in the growth (z) direction are shown. Dashed curve—anion p-orbital interface component. Solid curve—cation s-orbital Kronig-Penney component.

F_s is the envelope function of the s-orbital Kronig-Penney—type component, and F_p is the envelope function of the interfacial p-orbital component. Equation (7) of Ref. 9 provides a relationship between the amplitudes F_p and F_s of the two envelope functions which can be written as

$$F_p F_s = (E_g \hbar^2 k^2 / 2m^*)^{1/2} / E \ , \tag{5}$$

where E_g is the HgTe negative band gap (≈ 0.3 eV), m^* is the HgTe conduction-band effective mass, E is the energy of the superlattice state relative to the HgTe conduction-band edge, and k is the wave vector of a HgTe Bloch state with energy E. The ratio depends only the superlattice-state energy and not directly on the thicknesses of the HgTe and CdTe layers. For small energies E the ratio reduces to just $(E_g/E)^{1/2}$.

Figure 5 illustrates the interfacelike nature of the superlattice conduction-band minimum states. A simpler two-band tight-binding model was used to calculate the wave functions here.[10] This model includes the p orbitals on the anions (dashed line) and the s orbitals on the cations (solid line) only. Orbitals omitted by the model, such as s orbitals on anions and p orbitals on cations, produce approximately a 10% correction to the wave function and a 1% correction in the energy. The two superlattices shown have 40-Å—40-Å and 100-Å—100-Å thicknesses for the HgTe-CdTe layers at 4 K. The energy of the conduction-band-minimum state for the 40-Å—40-Å superlattice is 0.179 eV and that for the 100-Å—100-Å superlattice is 0.041 eV. Smaller energies produce higher interface amplitudes, as can be seen in agreement with Eq. (5).

VI. CONCLUSIONS

The multiband tight-binding method has been used to calculate the detailed subband energy dispersion of the HgTe-CdTe superlattice. Strain effects are incorporated and duplicate the results of the standard Bir-Pikus theory well for bulk HgTe. The semiconducting (111) superlattice band structure investigated here is found not to be significantly influenced by strain. Strain for the semiconducting (001) case reverses the order of the light- and heavy-hole subbands, resulting in a [001] hole effective mass lighter than expected if the heavy-hole band were higher. The in-plane hole mass of the (111) superlattice is significantly decreased as compared to the bulk heavy-hole mass, but only over a small range of energy. It is inconclusive whether or not this may contribute to the observed large mobilities.

Strain is found to significantly affect the band structure of the semimetallic superlattice investigated here. The light- and heavy-hole subbands are reversed and the effective masses and Fermi level modified from the unstrained values. Although the 40-meV offset rule is used here, the effect of strain implies that a redetermination is necessary.

The interface character of the conduction-band-minimum state is found to vary with energy, increasing for lower-energy states found in superlattices with thicker HgTe layers and smaller band gaps. A simple formula estimates the ratio of interface to Kronig-Penney amplitude in the wave function.

ACKNOWLEDGMENTS

Helpful discussions with G. Bastard, Y. R. Lin-Liu, T. C. McGill, G. Osbourn, K. V. Vaidyanathan, and G. Wu are gratefully acknowledged.

[1] J. N. Schulman and T. C. McGill, Appl. Phys. Lett. **34**, 663 (1979).
[2] D. L. Smith, T. C. McGill, and J. N. Schulman, Appl. Phys. Lett. **43**, 180 (1983).
[3] J. P. Faurie, A. Million, and J. Piaguet, Appl. Phys. Lett. **41**, 713 (1982).
[4] P. P. Chow and D. Johnson, J. Vac. Sci. Technol. A **3**, 67 (1985).

[5]Y. Guldner, G. Bastard, J. P. Vieren, M. Voos, J. P. Faurie, and A. Million, Phys. Rev. Lett. **51**, 907 (1983).

[6]J. P. Faurie, M. Boukerche, S. Sivananthan, J. Reno, and C. Hsu, in Proceedings of the International Conference on Superlattices, Microstructures, and Microdevices, Champaign, 1984 [Superlattices Microstruct. 1, 237 (1985)].

[7]C. E. Jones, T. N. Casselman, J. P. Faurie, S. Perkowitz, and J. N. Schulman, Appl. Phys. Lett. **47**, 140 (1985).

[8]S. Hetzler, J. P. Baukus, A. T. Hunter, J. P. Faurie, P. P. Chow, and T. C. McGill, Appl. Phys. Lett. **47**, 260 (1985).

[9]G. Bastard, Phys. Rev. B **25**, 7584 (1982).

[10]J. N. Schulman and Y.-C Chang, Appl. Phys. Lett. **46**, 571 (1985).

[11]Y. Guldner, G. Bastard, and M. Voos, J. Appl. Phys. **57**, 1403 (1985).

[12]G. Wu, C. Mailhiot, and T. C. McGill, Appl. Phys. Lett. **46**, 72 (1985).

[13]G. Wu and T. C. McGill, Appl. Phys. Lett. **47**, 634 (1985).

[14]Y.-C. Chang, J. N. Schulman, G. Bastard, Y. Guldner, and M. Voos, Phys. Rev. B **31**, 2557 (1985).

[15]Y. R. Lin-Liu and L. J. Sham, Bull. Am. Phys. Soc. **30**, 266 (1985); N. A. Cade, J. Phys. C **18**, 5135 (1985).

[16]D. J. Olego, J. P. Faurie, and P. M. Raccah, Phys. Rev. Lett. **55**, 328 (1985).

[17]G. Wu and T. C. McGill, J. Appl. Phys. **58**, 3914 (1985).

[18]P. W. Kruse, in *Semiconductors and Semimetals,* edited by R. K. Willardson and A. C. Beer (Academic, New York, 1981), Vol. 18, p. 1.

[19]J. N. Schulman and Y.-C. Chang, Phys. Rev. B **31**, 2056 (1985); Y.-C. Chang and J. N. Schulman, *ibid.* **31**, 2069 (1985).

[20]R. Dornhaus and G. Nimtz, *Narrow Gap Semiconductors* (Springer-Verlag, Berlin, 1983), p. 198.

[21]P. Lawaetz, Phys. Rev. B **4**, 3460 (1971).

[22]L. S. Dang, G. Neu, and R. Romestain, Solid State Commun. **44**, 1187 (1982).

[23]G. Milchberg, K. Saminadayar, E. Molva, and H. R. Zelsmann, Phys. Status Solidi B **125**, 795 (1984).

[24]G. C. Osbourn, J. Appl. Phys. **53**, 1586 (1982).

[25]G. Simmons and H. Wang, *Single Crystal Elastic Constants and Calculated Aggregate Properties: A Handbook,* 2nd ed. (The MIT Press, Cambridge, MA 1971).

[26]R. Yoshizaki and S. Tanaka, J. Phys. Soc. Jpn. **42**, 1601 (1977).

[27]J. W. Matthews and A. E. Blakeslee, J. Vac. Sci. Technol. **14**, 989 (1977).

[28]B. J. Roman and A. W. Ewald, Phys. Rev. B **5**, 3914 (1972).

[29]G. L. Bir and G. E. Pikus, Fiz. Tverd. Tela (Leningrad) **3**, 3050 (1961) [Sov. Phys.—Solid State **3**, 2221 (1962)]; M. Chandrasekhar and F. H. Pollak, Phys. Rev. B **15**, 2127 (1977); H. Mathieu, P. Merle, E. L. Ameziane, B. Archilla, and J. Camassel, Phys. Rev. B **19**, 2209 (1979). The last two provide convenient formulas.

[30]D. J. Chadi and M. L. Cohen, Phys. Status Solidi B **68**, 405 (1975); K. C. Hass, H. Ehrenreich, and B. Velický, Phys. Rev. B **27**, 1088 (1983), gives a version with misprints corrected.

[31]Y.-C. Chang, Phys. Rev. B **25**, 605 (1982).

[32]J. N. Schulman and Y.-C. Chang, in Proceedings of the Second International Conference on Modulated Semiconductor Structures, Kyoto, 1985 [Surf. Sci. (to be published)].

[33]G. C. Osbourn, in Proceedings of the International Conference on Superlattices, Microstructures, and Microdevices, Champaign, 1984 [Superlattices Microstruct. 1, 223 (1985)]; G. C. Osbourn (unpublished).

[34]J. C. Slater and G. F. Koster, Phys. Rev. **94**, 1498 (1954); D. J. Chadi, *ibid.* B **16**, 790 (1977).